УДК 620.197

Hongyan Cao [1,2], Xizhang Chen[2], Sergey Konovalov[3]

[1]School of Material Science and Engineering, Jiangsu University

[2]School of Mechanical and Electrical Engineering, Wenzhou University

[3]Department of Metals Technology and Aviation Materials, Samara National Research University

CORROSION BEHAVIOR OVERVIEW AND ANALYSIS OF CLAM STEEL VS. WELDMENTS IN LIQUID LITHIUM LEAD AT 753K*

Liquid lithium lead material is one of the most promising concepts for the latest fusion reactor blanket design which has been widely investigated. It uses liquid lithium lead as breeding material, lithium for neutron breeding and lead for producing tritium. China, the European Union, the United States and other members of ITER (International Thermonuclear Experimental Reactor) all pay significant attention to the research and development of the liquid lithium lead [1–3]. The main functions of the lithium lead alloy include energy conversion, tritium breed and radiation shield, it is crucial component in order to make fusion energy to achieve the ultimate applications. However, the concern about liquid metal blanket is its compatibility with candidate structural materials [4].

Coolant materials not only suffer high temperature and high pressure, but also bear strong neutron irradiation under complex dynamic condition. Reduced activation ferritic/martensitic (RAFM) steel used as structural materials becomes one of the most attractive designs for ITER-TBM [5]. To keep pace with the research and development of RAFM steel in other countries and meet the demands of constructing the DEMO and the first fusion power plant, China has developed its own low activation martensitic (CLAM) steel one of the RAFM (F82H, JLF-1, EUROFER 97, 9Cr2WVTa) steels, the research and development are done by the fusion design study team form ASIPP (Institute of Plasma Physics Chinese Academy of Sciences) in cooperation with some institutions and universities in 2001 [6]. CLAM steel serve as nuclear fusion reactor cladding material, is used for manufacturing TBM (Test Blanket Module) internal cooling passages [7], due to the flow channels structure is complex, different runner sizes and positions make overall molding difficult, welding technique is a major means of connecting these parts. The severe working conditions give strict requirements to CLAM steel and its weldments, therefore, improving the weld joint corrosion resistance is one of key factors in practical application. In this article, previous work on corrosion behavior between base metal and its weldments in static and flowing liquid lithium lead are focused.

Weldability of CLAM steel

Base on the research and design experience of Europe, Japan and United States about RAFM steel, China has developed its own characteristic, composition and performance optimized China Low Activation Martensitic steel. CLAM steel is regarded as one of the most realistic fusion first wall material, because of its excellent performance such as high resistance to irradiation swelling and irradiation embrittlement [8], low thermal expansion coefficient and high temperature mechanical properties compare to traditional austenitic stainless steels [9], Main chemical composition and mechanical properties are shown in Table 1 and Table 2, elements Nb and Mo that cause long time activation under neutron irradiation are replaced by W, V and Ta, the content of Ta is 0,20 % to improve the high temperature performance, Cr content at 9 % provides the lowest DBTT (ductile-brittle transition temperature) in irradiate condition, when the percentage is more than 12 %, delta ferrite will begin to appear, toughness will decrease and the corrosion rate will also be affected. The heat treatment is normalizing at 1253 K for 30 minutes and then cooling in air to room temperature (RT) and tempering at 1033 K for 90 minutes then air cooling to RT [17, 18]. After normalizing, high density dislocation structure is obtained, in subsequent tempering process the dislocation is reduced greatly and precipitated phase formed. These precipitates strongly pin in dislocations, further improve the high temperature mechanical properties, plasticity and toughness.

* This work is sponsored by the National Natural Science Foundation of China under Grant Nos. 50905079 and 51375216. We deeply acknowledge and appreciate the work our predecessors have done. We appreciate Professor Bruce Madigan and Mr. Nathan Huft from Montana Tech. for their language polishing.

Table 1

Chemical composition of RAFM steel [10 – 12] (wt %)

	Cr	W	V	Ta	Mn	C	Ni	Cu	Fe
CLAM	8.91	1.44	0.16	0.20	0.35	0.12	0.043	0.028	Bal
EUROFER 97	8.82	1.09	0.20	0.13	0.47	0.11	0.02	-	Bal
JLF-1	8.93	1.96	0.21	-	0.64	0.10	0.49	-	Bal

Table 2

CLAM steel mechanical properties between room temperature and 550℃ [13 – 16]

	Yield strength/MPa	Tensile strength/M	Elongation at fracture/%	Reduction of area/%	T_{DBTT}/℃
RT	512	660	23	77	-52
550℃	340	365	24	84	-

Microstructure is observed by optical microscope (OM) as shown in Fig. 1 [19]. Fig. 1 (*a*) shows that base metal microstructure distribution is uniform, grains refinement and no delta ferrite is observed, which means that base metal is fully tempered. After welding, microstructure is unevenly distributed, grain size become coarse as shown in Fig. 1 (*b*).

Suitable fusion welding technique for CLAM steel include gas tungsten arc welding (GTAW), laser beam welding (LBW), plasma arc welding (PAW), ultrasonic TIG welding and hot isostatic pressure diffusion welding (HIP) [20, 21]. The welding heat input, weld metal remelting and crystallization, heat affected zone (HAZ) grain growth, delta ferrite appear between the prior austenite grain boundaries have seriously affected the performance of the weldment [22 – 24]. These changes make weld joints prone to phenomenon of weld zone hardening, heat affected zone softening, and cold cracking. The advantages of GTAW method are: weld zone is well protected, heat input is concentrated and welding deformation is small as well as easily realize mechanization and automation. Beijing university of science and technology had done Y-type and double Y-type grooves welding tests on 13 mm thick CLAM steel plates using GTAW method [25], the study find that heat affected zone is slightly large, from fusion zone to base metal, hardness distribution firstly decrease and then slightly increase. GTAW welding of 4 mm thick CLAM steel is conducted with the current 96A and the speed is about 5cm/min in Jiangsu university [26], the results show that weld zone hardness values are on the high side, heat affected zone near the base metal existed a narrow softening area, microstructures are obvious lath character tempered martensite.

Liquid metal lithium lead loop

A series of experimental devices (heat convection and forced convection loop) on materials cor-

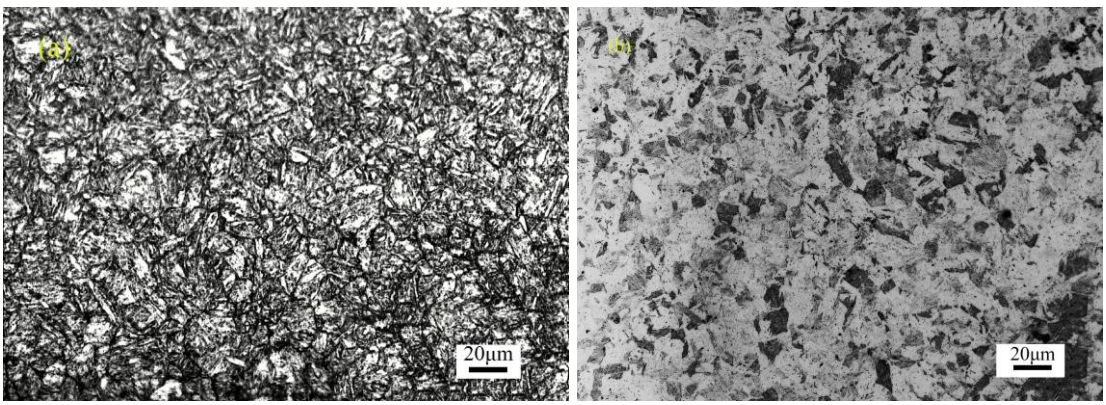

Fig. 1. Microstructure of base metal (*a*) and the weld (*b*) [19]

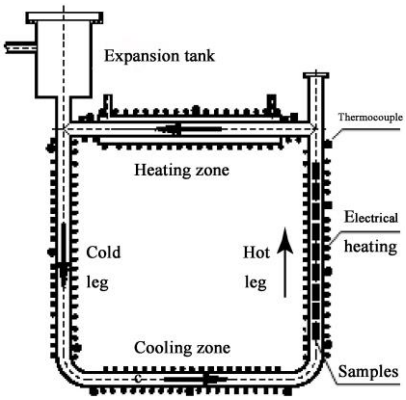

Fig.2. Schematic diagram of DRAGON-I loop. [2, 32]

rosion experiments in liquid lead lithium have been designed all over the world, and RAFM steel compatibility with liquid lithium lead is evaluated and validated [27 – 29]. In China FDS team [30, 31] has successfully developed the first liquid lithium lead corrosion experiment loop DRAGON-1, which the material is 316 L stainless steel, its inner diameter is 22 mm and outside diameter 32 mm, partial schematic diagram as shown in Fig. 2. The whole circuit device main body consists of hot section (to place samples), cold section, heating side, cooling side and the expansion tank. Cold and hot section temperature were set at 693 K and 753 K, heating side temperature is heated from 693 K to 753 K continuously, while cooling side temperature is designed from 753 K drop down to 693 K. The difference of temperature within the hot and cold section causes the lithium lead density distribution is non-uniform, thus forming heat convection circulation under gravity.

When operating the circuit, liquid lithium lead flow into the loop from expansion tank at the top, heat convection circulation flow between hot section and cold section, the velocity is about 0.08 m/s. After the corrosion experiments, samples are taken out and cleaned in the solution CH_3COOH, H_2O_2 and C_2H_5OH (1:1:1) to remove the residual layers and other corrosion compounds on the surfaces until the weight remain constant, the samples then are grounded using sandpapers with a grids order of 180, 360, 600, 800, 1000, 1200 and mechanically polished by diamond polishing agent with a diameter of 0,5 – 1,25 μm. After fine grinding and polishing, the surfaces are smooth enough to observe subtle signs of corrosion. Sample surface and the cross section are tested by XRD, EDS and SEM analysis.

CLAM steel vs. weldment corrosion rate

Weight loss and corrosion depth following with time are usually used to evaluate the corrosion rate. Corrosion loss is determined by weight measurements using electro balance with an accuracy of 0,01 mg. Fig. 3 shows the weight loss and time curve of low activation ferritic/martensitic in flowing LiPb at 753 K, the straight line slope between two points represents the corrosion rate. CLAM steel corrosion rate exhibits a linear increase close to 2500 hours, the weight loss is 1,18 mg/cm2 as the corrosion time reaches 5000 hours. In the early corrosion period, due to the pre-existing of passivation layers, the weight loss is small and specimens do not enter the stable corrosion stage, until passivation layers lose protection effect. Eurofer97 and JLF-1 also show better compatibility with liquid LiPb in dynamic conditions.

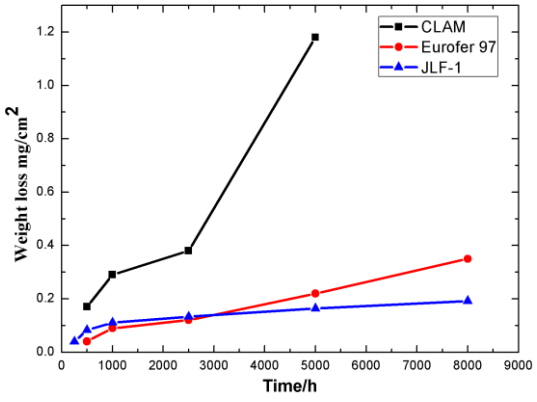

Fig. 3. Weight loss of low activation ferritic/martensitic steel as a function of time (Data are from Ref. 2, 4, 33, 34)

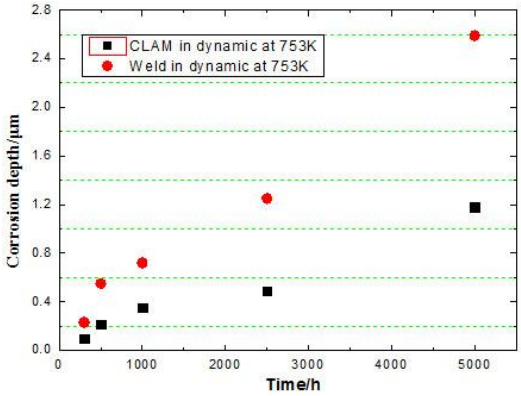

Fig.4. Corrosion rate comparison between CLAM steel and its weldments as a function of time (Data are from Ref. 1, 36, 37, 40)

Corrosion depth is influenced by various environmental parameters such as temperature, flow velocity and time [35]. The depth of the weldments increases with time and the corrosion rate is higher than that of base metal as shown in Fig. 4. When the exposing time was 2500 hours, corrosion depth of base metal is 0,5 μm and weld is 1,25 μm in dynamic conditions. Corrosion depth for 5000 h is calculated according to the previous existed corrosion rate. It is believed that the coarse martensite lath, residual stress, and high heat input under welding condition make the weldment corrosion resistance lower than base metal. If the high temperature leads to serious corrosion, the effect of flowing rate is greater. Therefore, the weld corrosion rate becomes more deserving research for long time under flowing LiPb conditions. Increasing the weldment corrosion resistance has a very important practical significance in order to improve the service life of structural blanket materials.

According to the above cases, if a nuclear reactor is designed for 100 years of operation, the CLAM steel base metal weight loss is about 206,74 mg/cm^2, the weld corrosion depth is about 438 μm, the numerical values are acceptable. That is to say China low activation martensite steel and its weld not only meet the requirements of the basic performance for common structural materials, and ensure the normal operation under service conditions.

CLAM steel vs. weldment surface investigation

Compared corrosion tests between CLAM steel and 316L stainless steel at 753 K with flow velocity 0,08 m/s in dynamic conditions for 500 h were conducted in the year 2005 by FDS team for the first time, SEM observation and EDS analysis had showed that CLAM steel corrosion resistance was better, the surface morphology and composition almost had no change [38]. Then longer time experiments of 2500 h in flowing LiPb were carried out, corrosive attack took place along the entire surface, the corrosion surface was inhomogeneous and started with the destroy of oxide layers formed during the heat treatment or specimens preparation process.

Chen et al [36] have studied and analyzed the corrosion behavior of CLAM steel under dynamic condition at 753 K in liquid lithium lead metal. Specimens surface morphology, chemical composition and corrosion rate had been observed and calculated. When the corrosion time approached 3000 hours, more than fifty percent of the specimen surface did not suffer attack, the probable reason was that the dense oxide layers protected the internal metal from dissolving into flowing lithium lead alloy. Analysis showed that no LiPb diffusion was detected on the surface and the maybe presence of ferritic phase reduced the corrosion resistance. Specimens that were exposed nearly 8000 hours exhibited irregular corrosion and the depth was approximately 15 μm as shown in Fig. 5. EDS line scan found major elements of Fe and Cr decreased greatly in the corrosion layer and the main difference was high oxygen content in the corrosion zone. Due to the diffusion effect, carbon element accumulated on the surface. As time changed longer, a newly formed chromium oxide layer with high level of oxygen began to appear under the corrosion layer, the thickness was about 10 μm. That was supposed, when exposure time was long enough, elements dissolving in liquid metal and the corrosion attack continued entering into the deeper matrix leaded to the destroy of the base metal and weight loss [39, 40]. Elements of Fe and Cr reduced near surface, the depleted layers thickness was around a few microns, elements such as oxygen, tungsten have improved obviously. Even though, the existence of protective layers did not prevent the metal from dissolving into liquid metal.

Due to the influence of weld heat input, heat affected zone (HAZ) near the fusion line or overheat region exhibited grain coarse, ultimately formed the coarse lath martensite structure, BSE

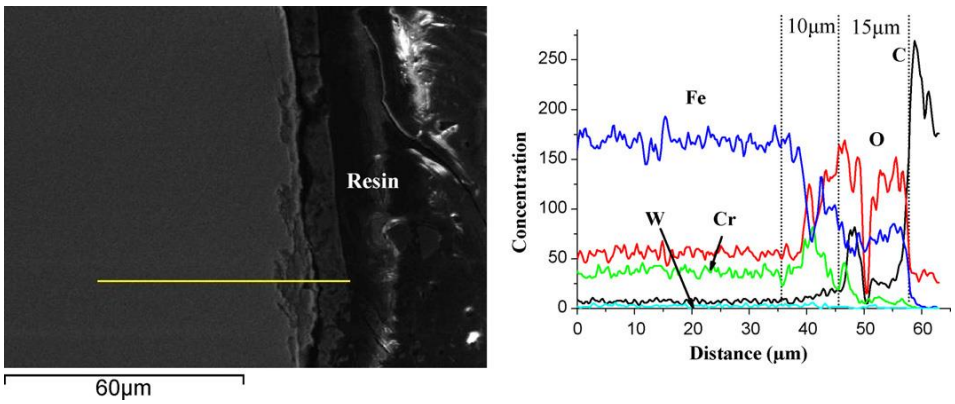

Fig. 5. Cross-section and EDS analysis after 8000 h exposure [38]

images as shown in Fig. 6. From weld metal (WM) to the coarse-grained heat affected zone (CGHAZ), uniform distributed micro-structure transformed to rough group. No carbide precipitations were found along the grain boundaries either in CGHAZ or fusion zone (FZ) of as-weld joint. Weld metal melting and solidification lead to the formation of similar casting structure. Because of high heat input and thermal cycle during GTAW process, the stress distribution was not uniform. The carbide particles or oxide scale formed on the original austenite grain boundary or the martensite lath boundary, chromium content was significantly reduced in this region, thus forming the easy corrosion area.

Microstructure of CLAM steel weld is usually coarse martensite and it has large quantities of residual stress, these factors generally have a great tendency to increase the corrosion attack, making the weldments become the weak area of the materials. According to Chen [40, 42] study, the test temperature was 753K with the flowing velocity 0,08 m/s, when the exposure time was less than 1000 hours, there was no lithium lead penetrating into CLAM steel weldment and the corrosion surface was uniform. It could be concluded that corrosion resistance of weld state was far lower than the tempered state of base metal, the coarse martensite lath in fusion zone gave rise to a high tend of corrosion.

Fig. 7. was XRD images after 3000 h exposure between base metal and weldment, it showed that curve peaks roughly in the same position of two pictures, which indicated that the main composition and phase had not changed, because there presented mostly tempered lath martensite and coarse martensite on the surface. The intensity of weldment at 2θ approach 45 degree was about 6500, while the base metal was 8000 [43, 44]. Fig. 8. showed corrosion morphology of CLAM steel GTAW weld joint, pitting corrosion could be observed clearly in Fig. 8, *a*. Fig. 8, *b* revealed when corrosion time was 1000 hours, corrosion degree was more serious than that of 500 hours. The gully like morphology had a parallel arrangement, the distances between the gullies were about 0,5 – 1 μm, a little thinner than the width of martensite lath. Weldment surfaces showed uniform corrosion and there were no lithium lead diffusing into internal metal, element of chromium between martensite laths separated out in form of chromium oxide or chromium carbide, at the places the original austenite grain boundary or the martensite lath were coarse produced chromium depleted area [42]. It was processing orientation and direction of martensite lath (DML) which were not absolutely vertical, that caused the chromium depleted area became more prone to corrosion.

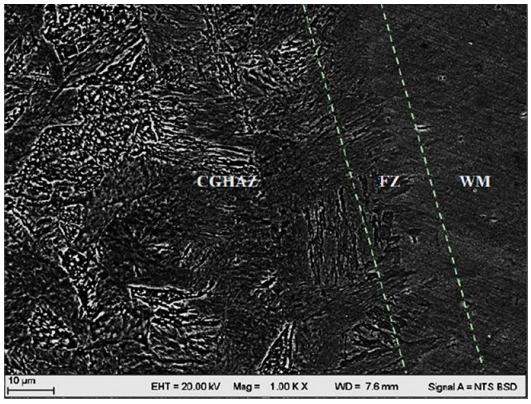

Fig. 6. BSE images near the CLAM weld [41]

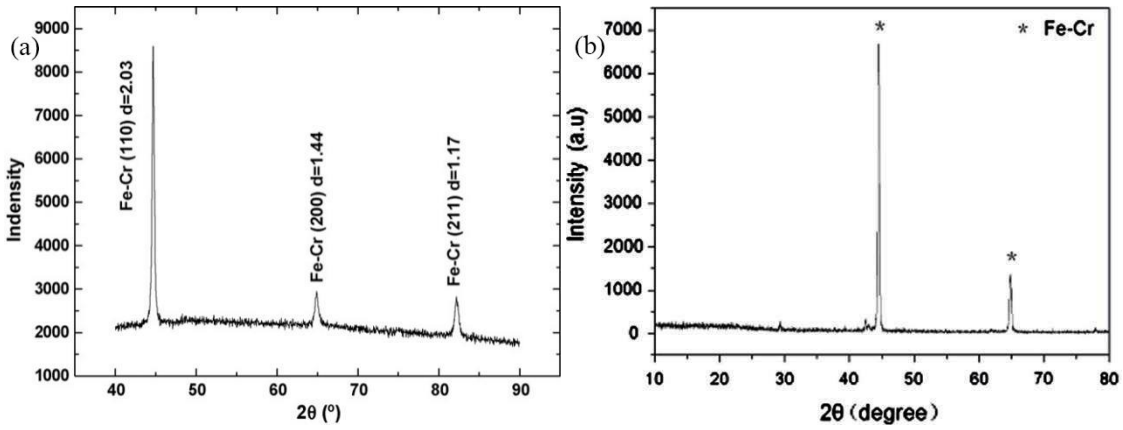

Fig. 7. XRD images after 3000 h exposure (*a*) base metal (*b*) weldment [43, 44]

When the direction of the martensite lath and the specimen surface presented small angle or near the grain boundary were more likely to become easy corrosion area. From the view of surface morphology, the easy corrosion area usually appeared along martensite lath. When exposing to liquid lithium lead, CLAM steel weldment enter into the stage of stable corrosion, at the same time there were more easy corrosion areas in contact with liquid metal, where as a result the initial corrosion rate was faster, weight loss was larger. Easy corrosion area presented peak and valley morphology with ups and downs. As long as the time increased, corrosion surface moved further inward to the internal steel.

Corrosion mechanism analysis

Dissolution and mass migration is the basic form for liquid metal corrosion, due to the difference between solubility and dissolution rate, elements selective dissolution occur in the liquid metal, mass migration refer to the directional movement and diffusion of metal material from one area to another. Based on previous research and analyses, the main corrosion mechanism for CLAM steel and its weldments in liquid lithium lead is the metal elements dissolving into the liquid LiPb and liquid metal penetrating into the solid structure materials [45]. Corrosion attack take place as a function of geometry, microstructure and composition. Prior precipitated austenite, martensite lath boundaries and areas with residual stress suffer severe corrosion [44]. Corrosion attack firstly dissolves pre-existing oxide layers formed in the process of tempering or heat treatment, the destruction requires a relatively long time, which is referred as the incubation period, and then corrosion continue to dissolve internal matrix and micro-alloy elements as shown in Fig. 9. The narrow yellow line stands for oxide layers, which is richer in chromium and depleted in metal iron, indicates that the oxide layers was likely $Cr_{23}C_6$ or Cr_2O_3. However, element of chromium in the matrix is depleted by diffusing to the liquid LiPb or forming the compounds [46, 47]. Elements diffusion to liquid metal as shown in Fig. 9, *b* and Fig. 9, *c*, the elements directional migration produce easy corrosion area and phase transformation. When the oxide layers are damaged, liquid LiPb alloy begin to permeate into base metal, reduce corrosion resistance of micro-structure, increase the weight loss of material and lead to severe corrosion.

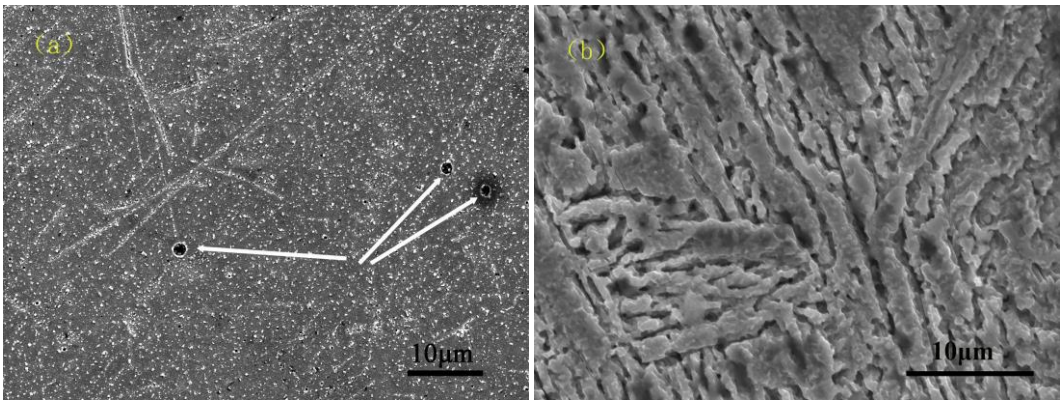

Fig. 8. Micrograph of CLAM steel weldments (*a*) after 500 h (*b*) after 1000 h [40]

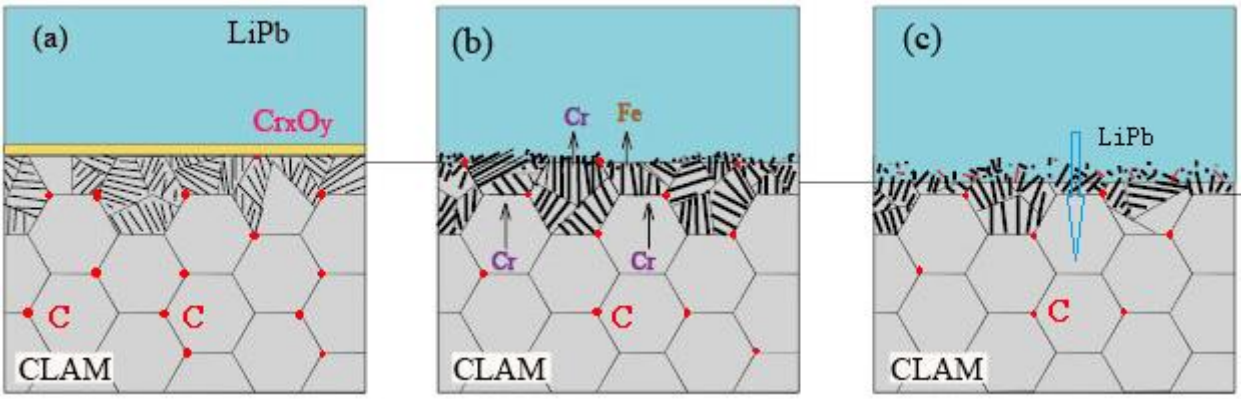

Fig.9. Corrosion behavior in flowing liquid LiPb (*a*) destroy of original oxides layer (*b*) alloy element dissolving (*c*) continuous dissolving and LiPb permeating

Compared with tempering treated CLAM steel, corrosion behavior of welding state is more serious, the probable reason may be related to the composition distribution and microstructure transformation. Base metal microstructure is mostly tempered lath martensite, filled with equiaxed sub-grains and a number of carbides precipitate on prior austenite grain boundaries, sub-grains boundaries and within martensite laths during tempering. While weld and heat affected zone microstructure is coarse, uneven distribution, similar to casting martensite, results in the decrease of corrosion resistance. Chemical composition differences between material internal and surface or grain boundary impurities and the existence of internal stress, component elements prior dissolving in liquid metal or liquid metal permeating along the grain boundary lead to grain boundary corrosion. Flow rate is too high or bend a sharp turn caused by liquid metal partial vaporization, similar to vacuum bubble forming, the surrounding liquid metal at high velocity flow into the bubbles impacting the material surface, as a result pitting occurs. These factors may cause serious corrosion, which needs further research in the subsequent experiments.

Conclusion. This paper provides a brief analysis on CLAM steel and its weldments corrosion behavior in liquid lithium lead at 753 K as well as a review of composition transmission, microstructures transformation and corrosion mechanism. Corrosion behavior under different temperature, flow rate and time in liquid metal need further study and conclusions are as follows:

CLAM steel corrosion behavior in flowing lithium lead at 753 K is overviewed, corrosion mechanism between CLAM steel and its weldment is concluded, the corrosion resistance of tempered base metal is superior to welds.

Corrosion rate exhibits a linear growth, weight loss increases with time, when the time reaches 5000 h, the weight loss is about 1,18 mg/cm^2, while the weldments weight loss is two times greater than that of the base metal, corrosion loss and depth are calculated for a long run.

Compositions and microstructures are compared, base metal surface is mostly presented by tempered lath martensite and weld zone microstructure is coarse, similar to casting martensite, corrosion resistance of coarse martensite is not as good as tempered one. XRD images showed that the peaks are rough at the same position (2θ) on the corrosion surface, weld surface has certain chromium content decreased, peaks intensity is weaker than in the base metal.

The presence of passivation (Fe – Cr oxides) layers has delayed wetting effect, which can effectively protect the internal base metal, reducing the corrosion rate at an early stage. Material elements dissolving and migrating into the liquid lithium are the main cause of the corrosion.

REFERENCES

1. Zhiqiang Zhu, Maolian Zhang, Sheng Gao, Yong Song, Chunjing Li et al, Preliminary experiments on the corrosion of CLAM steel in flowing eutectic LiPb. Fusion Engineering and Design, 200). Vol. 84 (1). P. 5-8.
2. Maolian Zhang, FDS Team. Corrosion experiment for CLAM and SS316L in liquid LiPb loop of China. Annals of Nuclear Energy, 2015, Vol. 80. P. 203-206.
3. Yanfen Li, Hiroaki Abe, Takuya Nagasaka, Takeo Muroga, Masatoshi Kondo. Corrosion behavior of 9Cr-ODS steel in stagnant liquid lithium and lead-lithium at 873 K. Journal of Nuclear Materials. 2013. Vol. 443. P. 200-206.
4. Qunying Huang, Sheng Gao, Zhiqiang Zhu, Maolian Zhang, et al. Progress in compatibility experiments on lithium–lead with candidate structural materials for fusion in China.

Fusion Engineering and Design, 2009. Vol. 84 (2-6). P. 242-246.

5. Zhihui Guo, Qunying Huang, Zilin Yan, Yong Song, Zhiqiang Zhu, et al. Compatibility of atmospheric plasma sprayed Al_2O_3 coatings on CLAM with liquid LiPb. Fusion Engineering and Design. 2010. Vol. 85. P. 1469–1473.

6. Qunying Huang, Chunjing Li, Qingsheng Wu, Shaojun Liu, Sheng Gao, et al, Progress in development of CLAM steel and fabrication of small TBM in China, Journal of Nuclear Materials, 2011. Vol. 417 (1-3). P. 85-88.

7. Ningshen S., Sakairi M., Suzuki K., Ukai S. The corrosion resistance and passive film compositions of 12% Cr and 15% Cr oxide dispersion strengthened steels in nitric acid media. Corrosion Science. 2014. Vol. 78. P. 322-334.

8. Lu Y.H., Wang Z.B., Song Y.Y., Rong L.J. Effects of pre-formed nanostructured surface layer on oxidation behaviour of 9Cr2WVTa steel in air and liquid Pb-Bi eutectic alloy, Corrosion Science. 2016. Vol. 102. P. 301-309.

9. Xizhang Chen, Yuming Huang, Bruce Madigan, Jianzhong Zhou, An overview of the welding technologies of CLAM steels for fusion application. Fusion Engineering and Design. 2012. Vol. 87. P. 1639-1646.

10. Konys J., Krauss W., Zhu Z. b, Huang Q. Comparison of corrosion behavior of EUROFER and CLAM steels in flowing Pb-15.7Li. Journal of Nuclear Materials. 2014. Vol. 455. P. 491-495.

11. Qi Xu, Masatoshi Kondo, Takuya Nagasaka, Takeo Muroga, Masaru Nagura, Akihiro Suzuki, Corrosion characteristics of low activation ferritic steel, JLF-1, in liquid lithium in static and thermal convection conditions. Fusion Engineering and Design. 2008. Vol. 83. P. 1477-1483.

12. Yanyun Zhao, Xiangwei Zhai, Shaojun Liu , Chunjing Li, Qunying Huang, High cycle fatigue properties of CLAM steel at 723K and 823K. Fusion Engineering and Design. 2015. Vol. 100. P. 608-613.

13. Shenghu Chen, Lijian Rong, Effect of silicon on the microstructure and mechanical properties of reduced activation ferritic/martensitic steel. Journal of Nuclear Materials. 2015. Vol. 459. P. 13-19.

14. Lixin Huang, Xue Hu, Chunguang Yang, Wei Yan, Furen Xiao, Yiyin Shan, Ke Yang, Influence of thermal aging on microstructure and mechanical properties of CLAM steel. Journal of Nuclear Materials. 2013. Vol. 443. P. 479-483.

15. Xue Hu, Lixin Huang, Wei Yan, Wei Wang, Wei Sha, Yiyin Shan, Ke Yang, Low cycle fatigue properties of CLAM steel at 823K. Materials Science&Engineering A. 2014. Vol. 613. P. 404-413.

16. Qunying Huang, FDS Team, Development status of CLAM steel for fusion application. Journal of Nuclear Materials. 2014. Vol. 455 (1-3). P. 649-654.

17. Qunying Huang, Qingsheng Wu, Shaojun Liu, Chunjing Li, Bo Huang, L. Peng et al. Latest progress on R&D of ITER DFLL-TBM in China. Fusion Engineering and Design. 2011. Vol. 86. P. 2611-2615.

18. Qunying. Huang, Chunjing. Li, Y. Li, M. Chen, Maolian. Zhang, L. Peng, Zhiqiang. Zhu, Yong. Song, Sheng. Gao. Progress in development of China Low Activation Martensitic steel for fusion application, Journal of Nuclear Materials. 2007. Vol. 367-370. P. 142-146.

19. Xizhang Chen, Yuanyuan Fang, Shuyan Zhang, Joe F. Kelleher, Jianzhong Zhou. Effects of LSP on micro-structures and residual stresses in a 4 mm CLAM steel weld joints. Fusion Engineering and Design. 2015. Vol. 94. P. 54–60.

20. Chunjing Li, Qunying Huang, Qingsheng Wu, Shaojun Liu, Yucheng Lei, et al. Welding techniques development of CLAM steel for Test Blanket Module. Fusion Engineering and Design. 2009. Vol. 84. P. 1184-1187.

21. Yuming Huang, Xizhang Chen, Zheng Shen, Bruce Madigan, Lei Yucheng, Jianzhong Zhou, Measurement and analysis of SHCCT diagram for CLAM steel. Journal of Nuclear Materials. 2013. Vol. 432. P. 460-465.

22. Xizhang Chen, Yuming Huang, Zheng Shen, J Chen, Lei Yucheng, Jianzhong Zhou, Effect of thermal cycle on microstructure and mechanical properties of CLAM steel weld CGHAZ. Science and Technology of Welding and Joining. 18 (4) 272-278.

23. Xizhang Chen, Zheng Shen, Jingjun Wang, et al, Effects of an ultrasonically excited TIG arc on CLAM steel weldjoints. International Journal of Advanced Manufacturing Technology. 2012. Vol. 60 (5-8). P. 537-544.

24. Qingsheng Wu, Shuhui Zheng, Shaojun Liu, Chunjing Li. Qunying Huang. Effect of post-weld heat treatment on the mechanical properties of electron beam welded joints for CLAM steel, Journal of Nuclear Materials. 2013. Vol. 442. P. 512-517.

25. Zhizhong Jiang, Litian Ren, Jihua Huang, Xin Ju, Huibin Wu, Qunying Huang, Yican Wu, Microstructure and mechanical properties of the TIG welded joints of fusion CLAM steel. Fusion Engineering and Design. 2010. Vol. 85. P. 1903-1908.

26. Yucheng Lei, Qiang Zhu , Ling Zhang , Kangjia Gu , Xin Ju, Simulation on the welding of CLAM steel. Fusion Engineering and Design. 2010. Vol. 85. P. 1503-1507.

27. Konys J., Krauss W., Voss Z., Wedemeyer O.. Corrosion behavior of EUROFER steel in flowing eutectic Pb–17Li alloy. Journal of Nuclear Materials. 2004. Vol. 329–333. P. 1379–1383.

28. Konys J., Krauss W., Voss Z., Wedemeyer O. Comparison of corrosion behavior of bare and hot-dip coated EUROFER steel in flowing Pb–17Li. Journal of Nuclear Materials. 2007. Vol. 367–370. P. 1144–1149.

29. Konys J., Krauss W., Novotny J., Steiner H., Voss Z., Wedemeyer O. Compatibility behavior of EUROFER steel in flowing Pb-17Li, Journal of Nuclear Materials. 2009. Vol. 386–388. P. 678–681.

30. Hongli Chen, Tao Zhou, Zhiyi Yang, Ruojun Lü, Zhiqiang Zhu, Mingjiu Ni, Magnetohydrodynamic experimental design and program for Chinese liquid metal LiPb experimental loop DRAGON-IV. Fusion Engineering and Design. 2010. Vol. 85. P. 1742–1746.

31. Yican Wu, FDS Team. Overview of liquid lithium lead breeder blanket program in China. Fusion Engineering and Design. 2011. Vol. 86. P. 2343–2346.

32. Sheng Gao, Maolian Zhang, Zhiqiang Zhu, Qunying Huang, Chunjing Li, et al. Preliminary experimental study on the corrosion of China low activation martensitic steel in liquid lithium lead. Chinese Journal of N uclear Science and Engineering. 2007. Vol. 27. P. 51-54.

33. Masatoshi Kondo, Minoru Takahashi, Teruya Tanaka, Valentyn Tsisar, Takeo Muroga, Compatibility of reduced activation ferritic martensitic steel JLF-1 with liquid metals Li and Pb-17Li. Fusion Engineering and Design. 2012. Vol. 87. P. 1777-1787.

34. Protsenko P., Terlain A., Jeymond M., Eustathopoulos N. Wetting of Fe-7.5%Cr steel by molten Pb and Pb-17Li. Journal of Nuclear Materials. 2002. Vol. 307-311. P. 1396-1399.

35. Konys J., Krauss W., Steiner H., Novotny J., Skrypnik A. Flow rate dependent corrosion behavior of Eurofer steel in Pb–15.7Li. Journal of Nuclear Materials. 2011. Vol. 417. P. 1191–1194.

36. Qunying Huang, Maolian Zhang, Zhiqiang Zhu, Sheng Gao. Corrosion experiment in the first liquid metal LiPb loop of China. Fusion Engineering and Design. 2007. Vol. 82. P. 2655–2659.

37. Sheng Gao, Qunying Huang, Zhiqiang Zhu, Zhihui Guo, Xinzhen Ling, Yaping Chen, Corrosion behavior of CLAM steel in static and flowing LiPb at 480℃ and 550℃. Fusion Engineering and Design. 2011. Vol. 86. P. 2627-2631.

38. Yaping Chen, Qunymg Huang, Sheng Gao, Zhiqiang Zhu, Xinzhen Ling, et al, Corrosion analysis of CLAM steel in flowingliquid LiPb at 480℃. Fusion Engineering and Design. 2010. Vol. 85. P. 1909-1912.

39. Glasbrenner H., Konys J., Röhrig H.D., Stein-Fechner K., Voss Z. Corrosion of ferritic-martensitic steels in the eutectic Pb-17Li. Journal of Nuclear Materials. 2000. Vol. 283-287. P. 1332-1335.

40. Xizhang Chen, Zheng Shen, Xing Chen, Yucheng Lei, Qunying Huang. Corrosion behavior of CLAM steel weldment in flowing liquid Pb-17Li at 480℃. Fusion Engineering and Design. 2011. Vol. 86. P. 2943-2948.

41. Junyu Zhang, Bo Huang, Qingsheng Wu, Chunjing Li, Qunying Huang. Effect of post-weld heat treatment on the mechanical properties of CLAM/316L dissimilar joint. Fusion Engineering and Design. 2015. Vol. 100. P. 334–339.

42. Xizhang Chen , Zheng Shen , Peng Li, Bruce Madigan, Yuming Huang , Yucheng Lei, et al, Compatibility of CLAM steel weldments with static LiPb alloy at 550℃. Fusion Engineering and Design. 2012. Vol. 87. P. 1565-1569.

43. Shaojun Liu, Qunying Huang, Chunjing Li, Bo Huang, Influence of non-metal inclusions on mechanical properties of CLAM steel, Fusion Engineering and Design, 2009. Vol. 84. P. 1214–1218.

44. Xizhang Chen, Qibing Yuan, Bruce Madigan, Wei Xue. Long-term corrosion behavior of martensitic steel welds in static molten Pb-17Li alloy at 550℃. Corrosion Science. 2015. Vol. 96. P. 178-185.

45. Yanfen Li, Hiroaki Abe, Takuya Nagasaka, Takeo Muroga, Masatoshi Kondo, Corrosion behavior of 9Cr-ODS steel in stagnant liquid lithium and lead-lithium at 873 K. Journal of Nuclear Materials. 2013. Vol. 443. P. 200-206.

46. Carsten Schroer, Olaf Wedemeyer, Josef Novotny, Aleksandr Skrypnik, Jürgen Konys, Selective leaching of nickel and chromium

from Type 316 austenitic steel in oxygen-containing lead-bismuth eutectic (LBE). Corrosion Science. 2014. Vol. 84. P. 113-124.

47. Yanfen Li, Hiroaki Abe, Takuya Nagasaka, Takeo Muroga, Masatoshi Kondo. Corrosion behavior of 9Cr-ODS steel in stagnant liquid lithium and lead–lithium at 873 K. Journal of Nuclear Materials. 2013. Vol. 443. P. 200–206.

Поступила 03 февраля 2017 г.

УДК 669:504.062.2′47

С.Н. Кузнецов, И.А. Рыбенко, Е.В. Протопопов, М.В. Темлянцев, С.В. Фейлер

Сибирский государственный индустриальный университет

ТЕРМОДИНАМИЧЕСКОЕ МОДЕЛИРОВАНИЕ ПРОЦЕССОВ ВОССТАНОВЛЕНИЯ ЖЕЛЕЗА ПРИ ТЕРМОХИМИЧЕСКОМ ОКУСКОВАНИИ КОНВЕРТЕРНЫХ ШЛАМОВ

Анализ перспектив развития сталеплавильного производства показывает, что в настоящее время наблюдается отчетливая тенденция более широкого применения при выплавке стали в дуговых сталеплавильных печах и конвертерах подготовленных шихтовых материалов, характерными представителями которых являются синтиком и оксидно-угольные брикеты [1, 2]. Фактически такие подготовленные шихтовые материалы представляют собой композиции из Fe – C – O-содержащих природных и техногенных материалов, в том числе окалины, шламов, плавильной пыли, коксовой мелочи и т.п. Синтетические композиционные материалы, являющиеся компонентами шихты, имеют определенный гранулометрический состав и форму. Весьма важным фактором является то, что Fe – C – O-содержащие композиционные шихтовые материалы кардинально меняют течение физико-химических процессов в сталеплавильной ванне. Это происходит благодаря наличию в их составе окислительных и восстановительных компонентов, которые соответствующим образом проявляются в различные периоды плавки [1].

В оксидноугольных брикетах восстановитель и окислитель смешаны до начала взаимодействия и, таким образом, подготовлены к реакции между углеродом и кислородом [1]. При этом мелкодисперстные железо- и углеродсодержащие компоненты обладают развитой поверхностью реагирования, что значительно интенсифицирует процессы восстановления.

К одной из разновидностей подготовленных или композиционных шихтовых материалов можно отнести феррококс и феррококсовые брикеты [3 – 5]. Концепция производства феррококса разработана еще в 30-х годах прошлого века и была ориентирована на спекание железорудной пыли, непригодной для плавки в доменных печах, с жирным или битуминизированным углем в коксовых батареях. Феррококс можно классифицировать как железоуглеродную композицию, прошедшую тепловую обработку вне плавильного агрегата. Феррококс – композиционный материал, содержащий в основном восстановленное железо и углерод. В работе [6] представлены результаты разработки основ технологии производства феррококса с применением адсорбционного обезвоживания и термохимического окускования конвертерных шламов. Завершающей стадией производства феррококса по такой технологии является термохимический способ окускования шлама в процессе его коксования в смеси со спекающимися углями. На этой стадии происходит восстановление железа из его оксидов. При этом практический интерес представляет определение термодинамических условий, необходимых для восстановления железа, и границ концентрационных областей, позволяющих рационализировать состав сырьевой смеси и температурный режим процесса.